2008

# An Experimental Study on Condensation of CO2 in a Horizontal Micro-fin Tube

Shigeru Koyama
*Kyushu University*

Chieko Kondou
*Hitachi Appliances*

Ken Kuwahara
*Kyushu University*

# An Experimental Study on Condensation of $CO_2$ in a Horizontal Micro-fin Tube

Shigeru KOYAMA [1]*, Chieko KONDOU [2] and Ken KUWAHARA [1]

[1] Faculty of Engineering Sciences, Kyushu University
6-1 Kasugakoen, Kasuga, Fukuoka, Japan
Phone: +81-92-583-7831, Fax: +81-92-583-7833

[2] Technology Development Department, Shimizu Air Conditioning Works, Hitachi Appliances, Inc.
390 Muramatsu, Shimizu, Shizuoka, Japan
Phone:+81-92-583-7831, Fax: +81-92-583-7833

## ABSTRACT

This paper deals with an experimental study on condensing characteristics of almost pure $CO_2$ in a horizontal micro-fin copper tube, which has a 5.67 mm equivalent inner diameter. The inside heat transfer coefficient, pressure drop, and void fraction were measured in the mass velocity ranging from 200 to 350 kg $m^{-2}$ $s^{-1}$ and the heat flux of 10 to 20 kW $m^{-2}$ at saturation pressures of 5.0 and 6.0 MPa. The experimental results show that the HTC changes moderately with the changing in mass flux and heat flux; however, the HTC increases significantly with the decrease in saturation pressure. In terms of pressure drop, though the effect of heat flux was negligible; it slightly increased in accordance with a decrease in saturation pressure. Also, the increase in mass velocity caused a significant increase in pressure drop. In addition, the present data was compared with previous correlations. The present data were significantly higher in heat transfer coefficient than these correlations. Hence, based on the present void fraction data the correlation of Koyama *et al*. has been modified and the modified correlation fits present data well.

## 1. INTRODUCTION

Helical micro-fin tubes have been commonly used in air conditioners. Thus, many investigations have been carried out for the heat transfer and the pressure drop characteristics of many hydrochlorofluorocarbons (HCFCs) and hydrofluorocarbons (HFCs) condensing in micro-fin tubes. For example, Koyama *et al*. (2006) have conducted an experimental investigation of R 22 and R 134a and proposed correlations for heat transfer coefficient (HTC), Goto *et al*. (2001) have measured the HTC and friction factor of R 410A, Cavallini *et al*. (2001) have investigated R 134a, R125a, R 32, R 410A and R 236ea, and Wang *et al*. (2002) have proposed a theoretical model on the condensation of R 11, R 123, R 134a, R 22 and R 410A in micro-fin tubes. However, from the viewpoint of the global environment protection, the natural refrigerant $CO_2$ has been recently applied to heat pump systems instead of HCFCs and HFCs. Also, it seems promising to utilize $CO_2$ in air conditioning and refrigeration systems. Therefore, it is valuable to confirm the condensation characteristics of $CO_2$ in a micro-fin tube.

In this work the condensation of $CO_2$ in a horizontal micro-fin tube is experimentally investigated, and the effects of mass velocity, heat flux and refrigerant saturation pressure on the heat transfer and pressure characteristics are discussed.

## 2. EXPERIMENTAL TECHNIQUE

### 2.1 Test loop and test section

Figure 1 shows a schematic diagram of the experimental refrigeration cycle. This cycle mainly consists of a compressor (1), an oil separator (2), a pre-cooler (3) a test section (4), an after-cooler (5), a receiver tank (6), an expansion valve (8) and electric heaters (9). Eight mixing chambers, for measuring refrigerant bulk temperature and pressure, are located next to each of the main elements in this cycle ; furthermore, the mass flow rate is measured with a Coriolis-type mass flow meter (7) located next to the receiver tank (6). The calibration accuracies of these sensors are listed in Table 1. Furthermore, the oil mass fraction was measured and found to be less than 0.1%.

Figure 2 shows a schematic view of the test section. The test section is made of two sections, one with water jackets for HTC and pressure drop measuring and the other for measuring the void fraction. The inside mean heat transfer coefficients in each water jacket segment, effective heat transfer length 520 mm and the pressure drop every 688 mm were measured. The vapor quality at the inlet of the test section was controlled by the pre-cooler. Furthermore, the mean void fraction in the 400 mm long adiabatic sampling section, next to condensing section, was measured using the quick closing valve method. Kondou *et al*. (2006) specifically described the procedures and data reductions of this method, thus they are omitted in this paper.

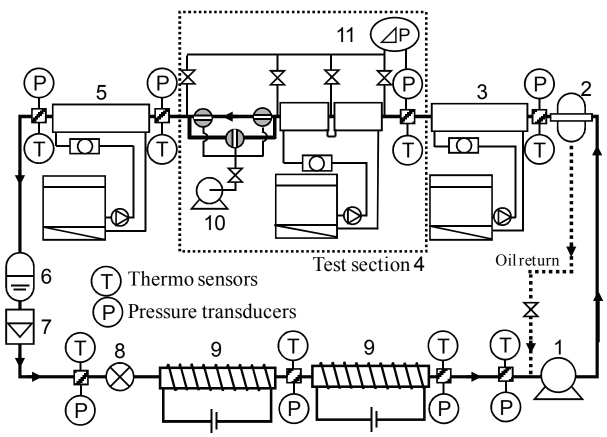


1 Compressor 5 After-cooler 9 Electric heaters
2 Oil separator 6 Receiver 10 Air compressor
3 Pre-cooler 7 Mass flow meter 11 Differential pressure transducer
4 Test section 8 Expansion valve

Figure 1: Schematic diagram of an experimental refrigeration cycle

Table 1: Calibration accuracies of sensors

| | |
|---|---|
| Refrig. bulk temp. | ± 0.05 K |
| Cooling water bulk temp. | ± 0.03 K |
| Tube outer surface temp. | ± 0.02 K |
| Refrig. pressure | ± 4.0 kPa |
| Refrig. pressure drop | ± 0.125 Pa |
| Refrig. mass flow rate after receiver | ± 0.28 kg/h |
| Cooling water volume flow rate | ± 1.0 l/h |
| Sampled refrig. Mass | ± 1.0mg |

Table 2: Experimental conditions

| № | Pressure | Mass flux | Heat flux |
|---|---|---|---|
| I | $P$=6.0 MPa | $G_r$=200 kg m$^{-2}$s$^{-1}$ | $q$=20 kW m$^{-2}$ |
| II | | | $q$=10 kW m$^{-2}$ |
| III | | $G_r$=350 kg m$^{-2}$s$^{-1}$ | $q$=20 kW m$^{-2}$ |
| IV | | | $q$=10 kW m$^{-2}$ |
| V | $P$=5.0MPa | $G_r$=200 kg m$^{-2}$s$^{-1}$ | $q$=20 kW m$^{-2}$ |

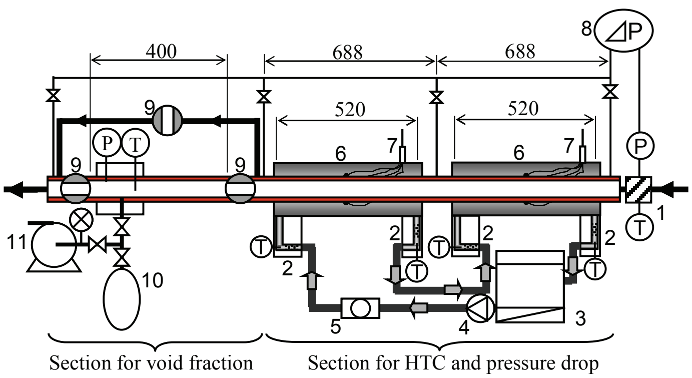


1 Mixing chambers for refrigerant
2 Mixing chambers for cooling water
3 Thermostatic bath
4 Pump for cooling water
5 Volume flow meter
6 Water jackets
7 Thermocouple on tube surface
8 Differential pressure transducer
9 Air actuated valves
10 Sampling vessel
11 Vacuum pump

Figure 2: Schematic view of test section

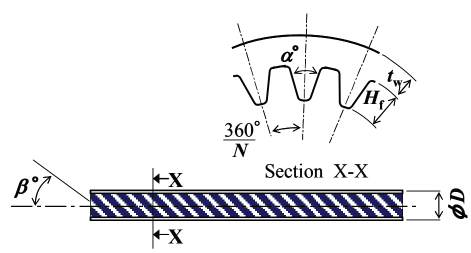


Figure 3: Dimensions of the test tube

Table 3: Dimensions of the test tube

| | | |
|---|---|---|
| O.D. | $D$ | 7.00 mm |
| Equivalent I. D. | $d_i$ | 5.67 mm |
| Thickness | $t_w$ | 0.60 mm |
| Fin height | $H_f$ | 0.23 mm |
| Number of fins | $N$ | 50 - |
| Apex angle | $\alpha$ | 30 ° |
| Helix angle | $\beta$ | 15 ° |
| Area increase ratio | $\eta$ | 184 % |

## 2.2 Experimental condition and test tube

As listed in Table 2, the experimental data was obtained in the mass velocity ranging from 200 to 300 kg $m^{-2}$ $s^{-1}$ at saturated pressures 5.0 and 6.0 MPa, in other words, the equally reduced pressure of 0.68 and 0.81. The averaged heat flux of both measurement sections (Section 1 and Section 2 in Fig. 4) was controlled at around 10 to 20 kW $m^{-2}$.

Table 3 lists the dimensions of this test tube, and Fig. 3 shows a schematic of these dimensions. Here, the equivalent I.D. signifies the inner diameter of an equivalent smooth tube with the same cross sectional area. The area increase ratio is the ratio of the extended heat transfer area inside the micro-fin tube to the inside heat transfer area of an equivalent smooth tube.

## 2.3 Data reduction method for central vapor quality and mean heat transfer coefficient

Figure 4 shows the estimation procedure of the central vapor qualities in each section. Specific enthalpy $h_{M1}$ is obtained from the bulk temperature and pressure of the superheated vapor in the mixing chamber at the entrance of pre-cooler. At the same time, pressure differences $\Delta P_{\alpha 1}(=P_1 - P_2)$, $\Delta P_{\alpha 2}(=P_2 - P_3)$ and $\Delta P_{void}(=P_3 - P_4)$, heat transfer rates $Q_{PC}$, $Q_{\alpha 1}$ and $Q_{\alpha 2}$, and refrigerant mass flow rate $W_r$ were measured. Here, these heat transfer rates of each section were obtained from the inlet and outlet bulk water temperature $T_{H2O,i}$ and $T_{H2O,o}$ as follows,

$$Q = \rho_{H2O} Cp_{H2O} V_{H2O} \left| T_{H2O,o} - T_{H2O,i} \right| - Q_{gain} \tag{1}$$

where $\rho_{H2O}$, $Cp_{H2O}$, and $V_{H2O}$ are density, specific heat, and volume flow rate of cooling water at an averaged temperature, respectively, and $Q_{gain}$ is the heat gain through the adiabatic materials surrounding the water jackets. The inlet and outlet vapor qualities of each section were obtained from specific enthalpy $h_1$ to $h_4$ and pressure $P_1$ to $P_4$ as shown in Fig. 4. Hence, the central vapor qualities could be expressed as the arithmetic average of the inlet and outlet. The heat flux is defined based on the actual heat transfer surface area inside the micro-fin tube as,

$$q = Q / \left( \pi d_i \Delta Z \eta_A \right) \tag{2}$$

The inside wall temperature is estimated by the following equation,

$$T_{wi} = T_{wo} - \left[ Q / \left( 2\pi \lambda_{tube} \Delta Z \right) \right] \ln \left( D / d_i \right) \tag{3}$$

Then, the HTC based on actual heat transfer area is defined as,

$$\alpha = q / \left( T_{sat} - T_{wi} \right) = Q / \left[ \pi d_i \Delta Z \eta_A \left( T_{sat} - T_{wi} \right) \right] \tag{4}$$

where $\Delta Z$ is the active condensation length of 520 mm, $\lambda_{tube}$ is the thermal conductivity of copper tube, $T_{wi}$ is the tube temperature at $d_i$, $T_{wo}$ is the tube temperature on the outer surface, and $T_{sat}$ is the refrigerant saturation temperature obtained from the refrigerant pressure $P_1$ to $P_3$.

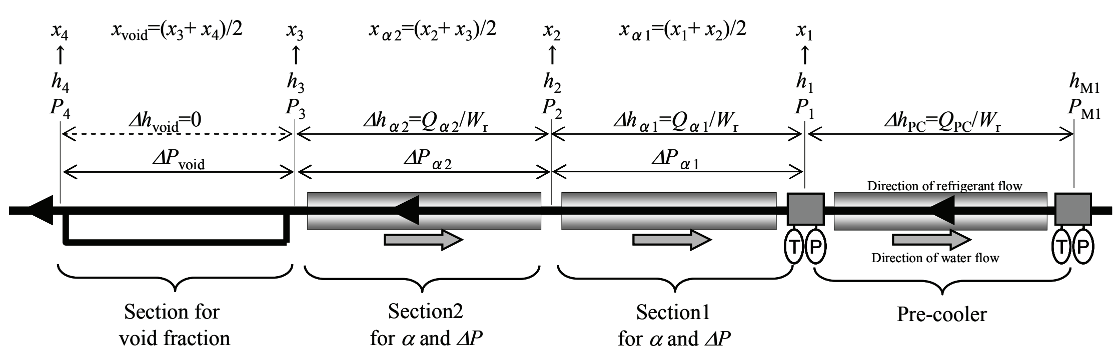

Figure 4: Estimation procedure for central vapor qualities in each section

# 3. RESULTS AND DISCUSSION

## 3.1 Experimental results on void fraction

Figure 5 shows the experimental results on void fraction with correlations at 5.0 and 6.0 MPa. Here the open symbols represent the void fraction and closed symbols represent the slip ratio found by the void fraction and density ratio of vapor to liquid. The solid lines are empirical correlations for boiling flow in micro-fin tubes proposed by Kondou *et al.* as given in Eqs. (4) to (6).

$$\xi = x \Big/ \left[ x + \left( s_{\rm M} + s_{\rm F} \right)\left(1-x\right)\left(\rho_{\rm G}/\rho_{\rm L}\right) \right] \tag{4}$$

$$s_{\rm M} = 0.4 + 0.6 \left[ \frac{1 + 0.4\left(\dfrac{1-x_{\rm v}}{x_{\rm v}}\right)}{\dfrac{\rho_{\rm G}}{\rho_{\rm L}} + 0.4\left(\dfrac{1-x_{\rm v}}{x_{\rm v}}\right)} \right]^{\frac{1}{2}}, \quad x_{\rm v} = \frac{x}{x + \left(1-x\right)\left(\rho_{\rm G}/\rho_{\rm L}\right)} \tag{5}$$

$$s_{\rm F} = 0.31 \left(\frac{1-x}{x}\right)^{-0.75} \left(\frac{\rho_{\rm G}}{\rho_{\rm L}}\right)^{-0.42} \left(\frac{\mu_{\rm L}}{\mu_{\rm G}}\right)^{0.35} \left(\frac{G_{\rm r}}{\sqrt{g d_h \rho_{\rm G}\left(\rho_{\rm L}-\rho_{\rm G}\right)}}\right)^{-0.78} \tag{6}$$

This correlation qualitatively agrees with the experimental results; however, the experimental slip ratio is lower than the correlation. For vapor quality below 0.2, the experimental slip ratio is lower than 1.0. This indicates that the vapor phase velocity is lower than that of the liquid phase and this feature on slip ratio causes increase of void fraction. Similar studies have been performed by Ahmed (1966) they use the term "wall void". For accidents, such as a slight gradient of the test tube or a bump near the orifice of the valves, bubbles were captured or delayed. However, in the following subsections, for estimating HTC and pressure drop, these characteristics are assumed to be negligible, and this correlation is applied to modify the previous correlation proposed by Koyama *et al.* (2006).

## 3.2 Experimental results on pressure drop and heat transfer coefficient

Figure 6 shows experimental results on pressure drop and HTC at conditions listed in Table 2. Open symbols represent the experimental results in Section 1 shown in Fig. 4 and closed symbols represent the experimental results in Section 2. The solid lines and dashed lines denote correlations later provided in subsection 3.3 and 3.4. The top figures show the results of heat flux $q$ and outside wall temperature $T_{\rm wo}$, the middle figures are results of pressure drop gradient $\Delta P/\Delta Z$, and the bottom figures are results of mean HTC $\alpha$. It is noted from the heat transfer diagram in Fig. 6 that the heat fluxes in both sections are not constant because the cooling water circuits are connected in series in the present study.

In terms of the pressure drop gradient, as shown in the comparison between Figs. 6 (a) and (c), the results at 6.0

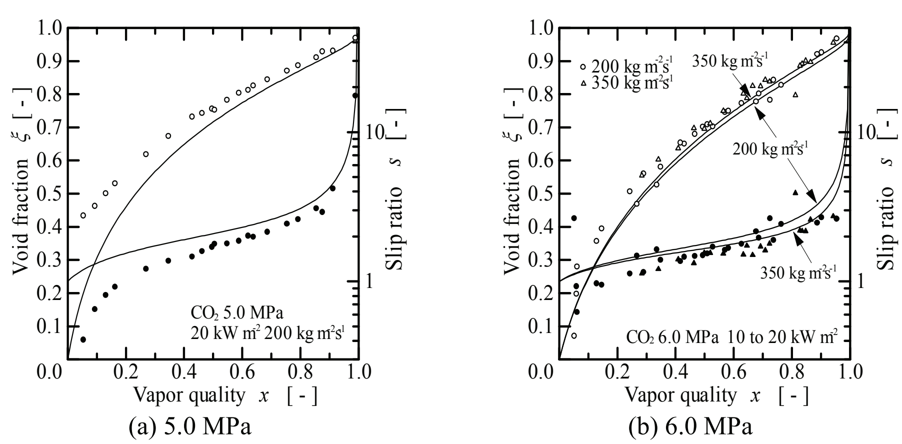


Figure 5: Experimental results on void fraction with present correlations

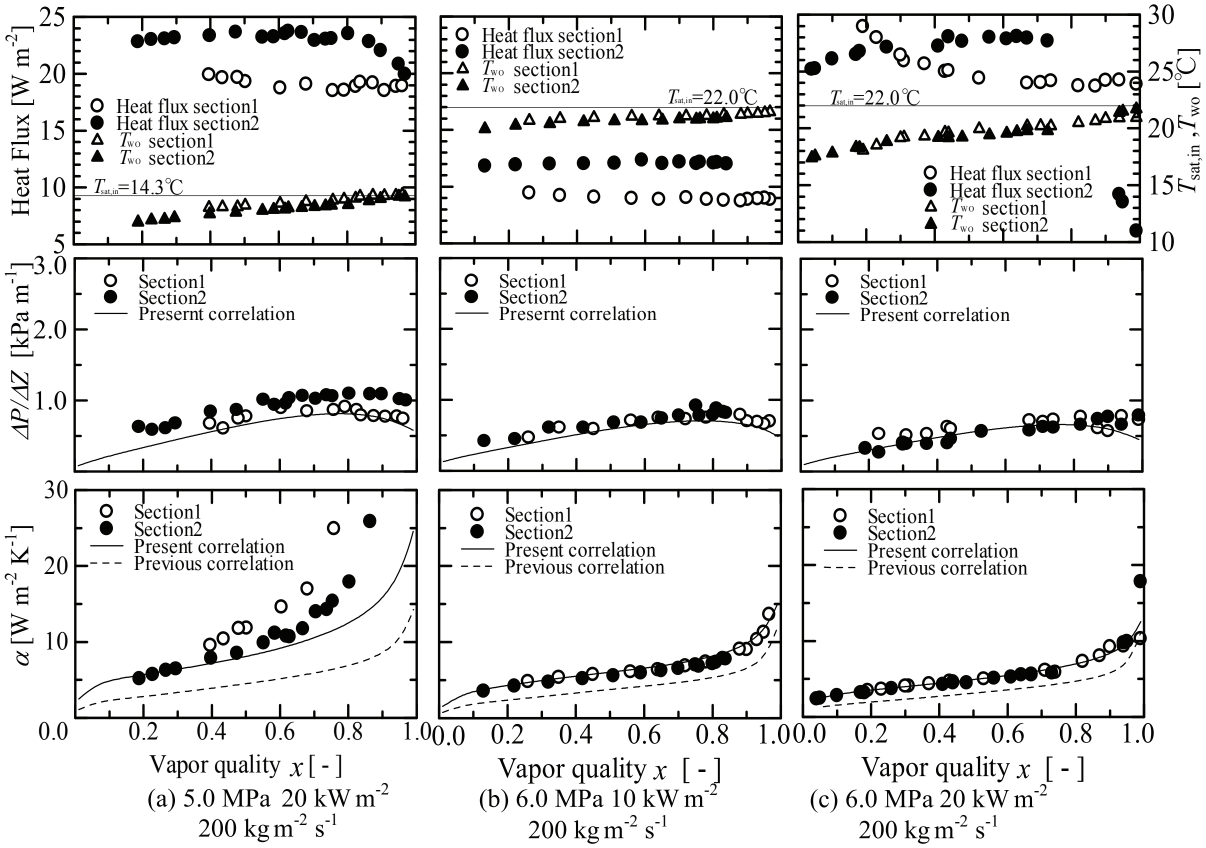


Figure 6: Experimental results on pressure drop and heat transfer coefficient with present correlations

MPa are lower than those at 5.0 MPa. This is mainly due to the difference in vapor density. As shown in the comparison between Figs. 6 (b) and (d) or (c) and (e), the pressure drop gradient significantly increases along with mass velocity. However, as shown in the comparison between Figs. 6 (b) and (c) or (d) and (e), the effect of heat flux is negligible.

In terms of HTC, as shown in the comparison between Figs. 6 (a) and (c), the results at 5.0 MPa are drastically higher than those at 6.0 MPa. This is mainly due to the difference in latent heat, that is, the latent heat at 5.0 MPa is lager than that at 6.0 MPa. In principle, Nusselt's filmwise condensation theory suggests that the value of HTC increases with the increase of latent heat. On the other hand, as shown in the comparison between Figs. 6 (b) and (d) or (c) and (e), the effect of mass velocity is negligible. This implies that the heat transfer characteristics are not dominated by the vapor shear stress near a critical point. As shown in the comparison between Figs. 6 (b) and (c) or (d) and (e), the effect of heat flux is also negligible.

### 3.3 Modified correlation for pressure drop

The static pressure drop can be expressed as a summation of momentum term and frictional term,

$$\Delta P = \Delta P_{\mathrm{M}} + \Delta P_{\mathrm{F}} \tag{7}$$

The pressure recovery due to momentum change $\Delta P_{\mathrm{M}}$ is given by,

$$\Delta P_{\mathrm{M}} = \left[ \frac{G_{\mathrm{r}}^{2} x^{2}}{\xi \rho_{\mathrm{G}}} + \frac{G_{\mathrm{r}}^{2} \left(1-x\right)^{2}}{\left(1-\xi\right) \rho_{\mathrm{L}}} \right]_{\mathrm{inlet}} - \left[ \frac{G_{\mathrm{r}}^{2} x^{2}}{\xi \rho_{\mathrm{G}}} + \frac{G_{\mathrm{r}}^{2} \left(1-x\right)^{2}}{\left(1-\xi\right) \rho_{\mathrm{L}}} \right]_{\mathrm{ontlet}} \tag{8}$$

As a trial, an empirical correlation for frictional pressure drop $\Delta P_{\mathrm{F}}$ is obtained from the present experimental results as,

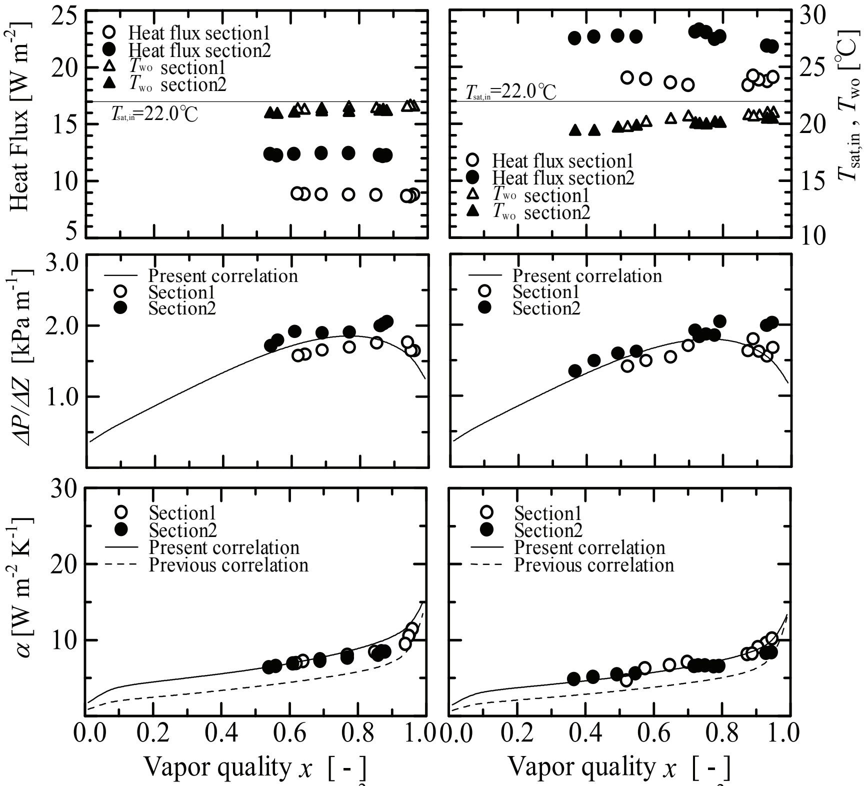


(d) 6.0 MPa 10 kW m$^{-2}$ 350 kg m$^{-2}$ s$^{-1}$ (e) 6.0 MPa 20 kW m$^{-2}$ 350 kg m$^{-2}$ s$^{-1}$

Figure 6: Continued

$$\frac{\Delta P_{\mathrm{F}}}{\Delta Z} = (1-x)\Phi_{\mathrm{L}}^{2}\left(\frac{\Delta P_{\mathrm{F}}}{\Delta Z}\right)_{\mathrm{L}} + x\Phi_{\mathrm{G}}^{2}\left(\frac{\Delta P_{\mathrm{F}}}{\Delta Z}\right)_{\mathrm{G}} \tag{9}$$

where,

$$\Phi_{\mathrm{L}} = 1.0 + 1.8 Fr^{0.01} X_{tt}^{-0.88} \tag{10}$$

$$\left(\frac{\Delta P_{\mathrm{F}}}{\Delta Z}\right)_{\mathrm{L}} = 4 f_{\mathrm{L}} \frac{G_{\mathrm{r}}^{2}(1-x)^{2}}{2 d_{\mathrm{i}} \rho_{\mathrm{L}}},\ f_{\mathrm{L}} = 0.046 Re_{\mathrm{L},d_{\mathrm{h}}}^{-0.2} \left(\frac{A_{\mathrm{cross,a}}}{A_{\mathrm{cross,n}}}\right)^{-0.5} \left(\sec\beta\right)^{-0.75} \tag{11}$$

$$\Phi_{\mathrm{G}} = 1.0 + 1.7 Fr^{0.01} X_{tt}^{0.55} \tag{12}$$

$$\left(\frac{\Delta P_{\mathrm{F}}}{\Delta Z}\right)_{\mathrm{G}} = 4 f_{\mathrm{G}} \frac{G_{\mathrm{r}}^{2} x^{2}}{2 d_{\mathrm{i}} \rho_{\mathrm{G}}},\ f_{\mathrm{G}} = 0.046 Re_{\mathrm{G},d_{\mathrm{h}}}^{-0.2} \left(\frac{A_{\mathrm{cross,a}}}{A_{\mathrm{cross,n}}}\right)^{-0.5} \left(\sec\beta\right)^{-0.75} \tag{13}$$

Here, $\Phi_{\mathrm{L}}$ and $\Phi_{\mathrm{G}}$ are t Martinelli's two-phase multipliers, respectively, relative to liquid and vapor. *Fr* is Froude number and $X_{\mathrm{tt}}$ is the Martinelli parameter for both phases in the turbulent regime. $f_{\mathrm{L}}$ and $f_{\mathrm{G}}$ are friction factors based on the nominal cross section area proposed by Carnavos (1980). The results predicted by the correlation, Eqs. (7) to (13), are represented by solid lines in the center of Fig. 6. Predicted results agree well with experimental results.

## 3.4 Modified correlation for heat transfer coefficients

The correlation for HTC, which was proposed by Koyama *et al*. (2006), is modified just a little based on the present experimental data. The results are expressed as,

$$Nu = \alpha\lambda_L / d_i = \left(Nu_{FC}{}^2 + Nu_{BF}{}^2\right)^{1/2} \tag{14}$$

$$Nu_{FC} = 2.12\left(\frac{\rho_L}{\rho_G}\right)^{0.1}\left(\frac{x}{1-x}\right)\Phi_G \cdot f_G{}^{0.5} Pr_L{}^{0.5} Re_{L,d_i}{}^{0.5} \tag{15}$$

$$Nu_{BF} = 3.12H(\xi)\eta_A{}^{-0.5} Bo^{-0.1}\left(Ga \cdot Pr_L / Ph\right)^{0.25} \tag{16}$$

$$H(\xi) = \xi + \left[10.0(1-\xi)^{0.17} - 8.9\right]\xi^{0.5}\left(1-\xi^{0.5}\right) \tag{17}$$

Where, $Nu_{FC}$ is the forced convective condensation term, $Nu_{BF}$ is the body forced convective condensation term, and $H(\xi)$ is the function expressing the active condensation area along the tube interior. In the present correlation, the coefficient in Eq. (16) is changed from 1.98 to 3.12, and the Galileo number $Ga$ is defined as,

$$Ga = \frac{g d_i^3}{\mu_L{}^2} \cdot \frac{(\rho_L - \rho_G)}{\rho_L} \tag{18}$$

Estimation results by the above correlation are shown at the bottom of Fig. 6. The solid lines represent the above modified correlation, and the dashed lines represent the previous correlation proposed by Koyama *et al*. (2006). From this figure, this modified correlation can be good for fitting to the experimental results. This modification is considered to be required because the density ratio of vapor to liquid increases under near-critical point conditions and the effect of body force relatively increase due to slowing vapor shear stress.

## 4. CONCLUSIONS

Experimental results on the heat transfer coefficient, pressure drop, and void fraction of $CO_2$ condensing flow in a horizontal micro-fin tube at 5.0 and 6.0 MPa were presented. The conclusions are as follows:

- Void fraction under near-critical point satisfactorily agreed with the correlation proposed by authors, even though bubble capture appeared similar to the wall void.
- The pressure drop obviously decreased with increase of refrigerant pressure, because the vapor shear stress decreased by the vapor density increasing.
- The condensing HTC decreased with increase of refrigerant pressure due to the change of latent heat.
- Prediction correlations for pressure drop and HTC, which are good for fitting this present data, have been proposed.

## NOMENCLATURE

| | | |
|---|---|---|
| $A_{cross,a}$ | actual cross sectional area | (m$^2$) |
| $A_{cross,n}=d_{i,n}{}^2\,\pi / 4$ | nominal cross sectional area | (m$^2$) |
| $d_i = (4A_{cross,a}/\pi)^{0.5}$ | equivalent tube inner diameter | (m) |
| $d_{i,n}=D-2t_w$ | nominal tube inner diameter | (m) |
| $d_h = (4A_{cross,a}) / (d_i\,\pi\,\eta_A)$ | hydraulic diameter | (m) |
| $\beta$ | helix angle of fin | (rad) |
| $\eta_A$ | heat transfer area enlargement | ( - ) |
| $T$ | temperature | (K) |
| $P$ | pressure | (Pa) |
| $G_r$ | mass flux | (kg m$^{-2}$ s$^{-1}$) |
| $h$ | bulk enthalpy | (J kg$^{-1}$) |
| $\Delta H$ | latent heat | (J kg$^{-1}$) |
| $C_p$ | isobaric specific heat capacity | (J kg$^{-1}$ K$^{-1}$) |
| $H(\xi)$ | active condensing area ratio | ( - ) |
| $\sigma$ | surface tension | (N m$^{-1}$) |
| $\mu$ | viscosity | (Pa s) |
| $\lambda$ | thermal conductivity | (W m$^{-1}$ K$^{-1}$) |

**Subscripts**

| | |
|---|---|
| in | inlet |
| out | outlet |
| H2O | cooling water |
| wi | equivalent inner diameter |
| wo | tube outside surface |
| sat | saturation |
| G | vapor |
| L | liquid |
| a | actual |
| n | nominal |
| T | total |
| M | momentum |
| F | frictional |
| FC | forced convection |
| BF | body force |

| | | |
|---|---|---|
| $\rho$ | density | (W m$^{-1}$ K$^{-1}$) |
| $g$ | gravitational acceleration | (m s$^{-2}$) |
| $\alpha$ | mean heat transfer coefficient | (W m$^{-2}$ K$^{-1}$) |
| $\Delta P$ | pressure drop | (Pa) |
| $\Delta P$ / $\Delta Z$ | pressure drop gradient | (Pa m$^{-1}$) |
| $\xi$ | void fraction | ( - ) |
| $s$ | slip ratio | ( - ) |
| $f$ | friction factor | ( - ) |
| $Nu = \alpha\, \lambda_{\mathrm{L}} / d_{\mathrm{i}}$ | Nusselt number | ( - ) |
| $Bo = [\, g\, d_{\mathrm{i}} (\rho_{\mathrm{L}}\text{-}\rho_{\mathrm{G}})] / \sigma$ | Bond number | ( - ) |
| $Fr = G_{\mathrm{r}} / [g\, d_{\mathrm{i}} \rho_{\mathrm{G}} (\rho_{\mathrm{L}}\text{-}\rho_{\mathrm{G}})]^{0.5}$ | Froude number | ( - ) |
| $Ph = [(T_{\mathrm{sat}} - T_{\mathrm{wi}})\, C_{\mathrm{p\,L}}] / \Delta H$ | phase change number | ( - ) |
| $Pr_{\mathrm{L}} = (C_{\mathrm{p\,L}}\, \mu_{\mathrm{L}}) / \lambda_{\mathrm{L}}$ | Prandtl number of Liquid phase | ( - ) |
| $Re_{\mathrm{L},di} = [G_{\mathrm{r}} (1\text{-}x)\, d_{\mathrm{i}}] / \mu_{\mathrm{L}}$ | liquid phase Reynolds number based on equivalent inner diameter | ( - ) |
| $Re_{\mathrm{L},dh} = [G_{\mathrm{r}} (1\text{-}x)\, d_{\mathrm{h}}] / \mu_{\mathrm{L}}$ | liquid phase Reynolds number based on hydraulic diameter | ( - ) |
| $Re_{\mathrm{G},dh} = (G_{\mathrm{r}}\, x\, d_{\mathrm{h}}) / \mu_{\mathrm{G}}$ | vapor phase Reynolds number based on hydraulic diameter | ( - ) |
| $\Phi_{\mathrm{G}} = [(\mathrm{d}P_{\mathrm{F}}/\mathrm{d}Z) / (\mathrm{d}P/\mathrm{d}Z)_{\mathrm{G}}]^{0.5}$ | Martinelli multiplier relative to vapor phase | ( - ) |
| $\Phi_{\mathrm{L}} = [(\mathrm{d}P_{\mathrm{F}}/\mathrm{d}Z) / (\mathrm{d}P/\mathrm{d}Z)_{\mathrm{L}}]^{0.5}$ | Martinelli multiplier relative to liquid phase | ( - ) |
| $X_{tt} = [(1 - x) / x]^{0.9} (\rho_{\mathrm{G}} / \rho_{\mathrm{L}})^{0.5} (\mu_{\mathrm{L}} / \mu_{\mathrm{G}})^{0.1}$ | Martinelli parameter relative to both phase | ( - ) |

## REFERENCES


Koyama, S., Yonemoto, R., 2006, Experimental study on condensation of pure refrigerants in horizontal micro-fin tube, *Proc. The 11 th Int. Refrig. and Air conditioning conf. at Purdue*, R133.

Carnavous, T. C., 1980, Heat transfer performance of internally finned tubes in turbulent flow, *Heat transfer engineering*, vol. 1, no.4, p.32-37

Kondou, C., Kuwahara, K., Koyama, S., 2008, An experimental study on condensation of $CO_2$ in a horizontal micro-fin tube, *Proc. The 12 th Int. Refrig. and Air conditioning conf. at Purdue*, (now printing).

Wang, H. S., Honda, H., Nozu, S., 2002, Modified theoretical models of film condensation in horizontal microfin tubes, *Int. J. Refrig.*, vol. 45, p.1513-1523.

Cavallini. A., Censi, G., Del Col, D., Doretti, L., Longo, G. A., Rossetto, L., 2001, Experimental investigation on condensation heat transfer and pressure drop of new HFC refrigerants, *Int. J. Refrig.*, vol. 24, p.73-87.

Goto, M., Inoue, N., Ishiwatari, N., 2001, Condensation and evaporation heat transfer of R 410A inside internally grooved horizontal tubes, *Int. J. Refrig.*, vol. 24, p.628-638.

Nusselt, W., 1916, Die Oberflachenkondensation des wasserdampfes, *Vereines Deutscher Ingenieure*, Vol. 60, no. 27, p.541-546.

Thome, J. R., 2005, Condensation in plane horizontal tubes: Recent advances in modeling of heat transfer to pure fluids and mixtures, *J. of the Boraz. Soc. of Mech. Sci. and Eng.*, Vol.27, no.1, p.23-30.

Koyama, S., Miyara, A., Takamatsu, H., Fujii, T., 1990, Condensation heat transfer of binary refrigerant mixture of R 22 and R 114 inside a horizontal tube with internal spiral grooves, *Int. J. Refrig.*, vol. 13, p.256-263.

Ahmad, S. Z., 1966, Axial distribution of bulk temperature and void fraction in a heated channel with inlet subcooling, *Trans. ASME*, Ser.C, Vol. 92, p.595-609.

Graham, D., Chato, J. C., Newell, T. A., 1999, Heat transfer and pressure drop during condensation of refrigerant 134a in an axially grooved tube, *Heat and mass transfer*, Vol. 42, p.1935-1944.


## ACKNOWLEDGEMENT


This investigation was partly supported by the Japan Refrigeration and Air conditioning Industry Association and the information of micro-fin tube was provided by Hitachi Cable, Ltd, which are gratefully acknowledged.